

## Transport and optical properties of low-resistivity CdSe

R. Tenne

*Department of Materials Research, Weizmann Institute of Science, Rehovot 76100, Israel  
and Laboratoire de Physique des Solides, Centre National de la Recherche Scientifique,  
1 place Aristide Briand, 92195 Meudon, France*

R. Jäger-Waldau, M. Lux-Steiner, and E. Bucher

*Fakultät für Physik, Universität Konstanz, D-7750 Konstanz, Federal Republic of Germany*

J. Rioux and C. Levy-Clement

*Laboratoire de Physique des Solides, Centre National de la Recherche Scientifique,  
1 place Aristide Briand, 92195 Meudon, France*

(Received 27 December 1989)

Transport and optical properties of *n*-type CdSe crystals together with microanalysis of residual impurities from two different sources (A and B) were investigated and compared in detail. It was found that the electronic properties of the crystals are governed by two kinds of shallow donors. At low temperatures ( $T < 150$  K) a shallow level 10 meV is dominating the transport properties, while at  $T > 150$  K a 22-meV level is the predominant one for crystal A. In addition, crystal B exhibits higher density of free carriers at all temperatures and the activation energy of its only shallow donor level is 10 meV. Laue patterns (x-ray measurements) showed that crystal B has a mosaic structure. Low-temperature photoluminescence spectra were measured for two crystals of A source, both low-resistivity *n* type (one undoped, the other In doped), and for crystal B. Two kinds of donors were identified in accordance with the transport measurements: one having an energy of about 10 meV, the other with energy of about 20 meV. The high-temperature photoluminescence of crystal B consisted of two peaks. They could be associated with emission from the A and B gaps of Wurzite-type crystals. Room-temperature photoluminescence measurements showed that the energy gap of crystal B is higher by 6 meV than that of crystal A, which was attributed to the strain in this crystal. The origin of the two shallow donor levels seen in the transport and photoluminescence measurements is discussed in light of the elemental microanalysis and the existing literature. We suggest that In is responsible for the 10-meV level, while the deeper level (20 meV) is attributed to Na.

### I. INTRODUCTION

CdSe is a wurtzite-type semiconductor belonging to the II-VI family of compounds. The applications of this material are for photovoltaic cells,<sup>1</sup> photoconductive materials,<sup>2</sup> thin-film transistors,<sup>3</sup> and optical-data recording.<sup>4</sup>

Transport properties<sup>5,6</sup> and photoluminescence<sup>7-13</sup> of CdSe were investigated by a number of groups in the past. Henry *et al.*<sup>8</sup> concluded that Li and Na are the only shallow acceptors on a substitutional site in CdSe besides P, which was supposed to form a shallow complex. Since it was not possible to make CdSe with *p*-type conductivity, it was suggested<sup>14</sup> that (a) the solubility of suitable shallow acceptors may be lower than the minimum background of donor impurities, and (b) the same kind of impurities which form the acceptors may also act as donors on different sites—or native defects may form electrically inactive complexes with the acceptor impurities.

Indium serves as a shallow donor in CdSe. However, no detailed investigation of this impurity in CdSe is reported in the literature (to the best of the author's knowledge). Alkali-metal impurities have been investigated in detail in ZnSe.<sup>15</sup> It was found that both Li and Na serve as shallow interstitial donors in this material.

On the other hand, substitution of the alkali atom with the Zn atom leads to a shallow acceptor state.

*n*-type CdSe has been studied extensively in photoelectrochemical cells. Thin films were prepared by a variety of techniques,<sup>16</sup> and their electronic and optical properties were not always fully characterized. Furthermore, their characteristics seem to depend strongly on the method of preparation. Therefore low-resistivity single-crystal *n*-type CdSe could serve as a reference for such investigations provided its electronic and optical properties were well characterized.

In the framework of this investigation, transport measurements, secondary-ion mass spectrometry (SIMS), electron-microprobe (EM), Laue x-ray-diffraction, photoluminescence (PL) at low temperatures, and optical measurements at room temperature were used to investigate the electronic properties of low-resistivity CdSe crystals.

### II. EXPERIMENT

Low-resistivity *n*-type CdSe single crystals (0001) oriented, were purchased from two manufacturers (A and B), and used in this investigation. All crystals were grown by the Bridgman technique under excess Cd vapor

pressure. Crystals specified with three different resistivities were purchased from manufacturer A designated A1 (0.3  $\Omega$  cm), A2 (1.0  $\Omega$  cm), and A3 (11  $\Omega$  cm). Extrinsic dopant (indium) was added to the melt deliberately in the case of crystal A1. Crystal B was specified as having a resistivity of 0.2  $\Omega$  cm. The crystals were polished down to a 1- $\mu$ m grit, etched in a mixture of concentrated HCl:HNO<sub>3</sub> (4:1), and finally cleaned in a 10% KCN solution. X-ray diffraction was performed in the Laue mode.<sup>17</sup> Beam diameter was about 1 mm. For the transport measurements four indium contacts were soldered onto one of the (0001) crystal faces in the van der Pauw geometry.

Transport properties were measured for crystals A1 and B between 40 and 340 K. The resistivity  $\rho$  and Hall mobility  $\mu$  were measured versus temperature  $T$ . The net carrier density  $N_{\text{eff}}$  was calculated via

$$N_{\text{eff}} = 1(\rho\mu e_0),$$

where  $e_0$  is the elementary charge.

Secondary-ion mass spectrometry was performed using a CAMECA IMS 3F spectrometer. The rate of sputtering, determined by a stylus, was 1  $\mu$ m/h. Electron-microprobe measurements were carried out using a CAMEBAX electron microprobe.

Photoluminescence was measured with a conventional setup equipped with a double grating high-resolution monochromator (Jobin-Yvon model HRD). The sample was immersed in a cryogenic helium bath (TBT). Excitation sources were the 514.4-nm eV line of an argon-ion laser (Spectra Physics model 2030), and the 647.1-nm (1.916 eV) line of a krypton-ion laser (Spectra Physics model 165). In all measurements the electric field ( $E$ ) of the beam was perpendicular to the specified  $c$  axis ( $E \perp c$ ) of the crystal.

Photocurrent spectra were measured at room temperature (300 K) in polysulfide solution. Calibration of the photoresponse was done by a UDT Si detector (model 260).

### III. RESULTS

#### A. Transport measurements

The results of the transport measurements at room temperature and at 80 K are summarized in Table I.

The resistivity ( $\rho$ ) versus temperature ( $T$ ) for crystal A1 (0.3  $\Omega$  cm), and for crystal B are shown in Fig. 1. The resistivity of crystal B decreases first upon increasing the temperature and exhibits a minimum at 100 K. Crystal A1 shows a different temperature dependence than crystal B. When the temperature is raised from 40 K the

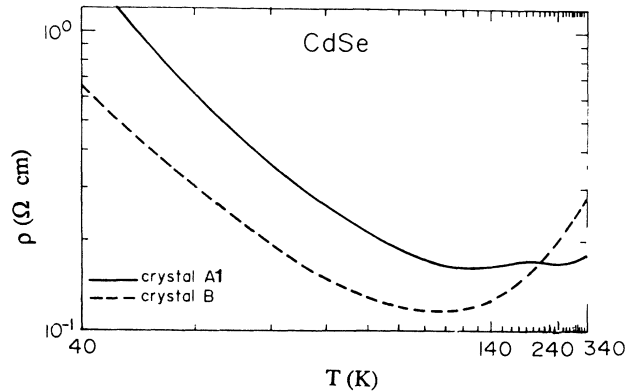


FIG. 1. Specific resistivity vs temperature for the two kinds of CdSe crystals (0.3- $\Omega$  cm A1 and B).

specific resistivity of crystal A1 goes down gradually and shows a first minimum between 120 and 130 K. Another minimum occurs around 250 K. It is likely that two minima are obtained as a result of the ionization of two different impurities. At low temperatures the shallow donor is ionized, while the deeper one is ionized above 250 K.

At about 130 K a maximum is reached in the mobility and thereafter it decreases with temperature as shown in Fig. 2. It was found that in the temperature range 120–340 K the mobility followed the power law  $\mu \propto T^{-1.15}$  for both crystals.

In the low-temperature range, where the exponent  $n$  is positive, it was not evaluated due to the lack of experimental data. The lower mobility of crystal B indicates that the density of free carriers is higher in crystal B than in crystal A1, which confirms the result of the numerical analysis. Note that the maximum in the mobility appears at somewhat higher temperature for crystal A1 than for crystal B, which is inconsistent with the previous conclusion. However, in view of the fact that the maximum is very broad, no firm conclusion is possible based on these data.

The density of free carriers ( $N_{\text{eff}}$ ) was determined experimentally and is shown in Fig. 3(a). The activation energy ( $E_A$ ) was graphically deduced from the dependence of  $N_{\text{eff}}$  on temperature  $T$  [Fig. 3(a)]. The following formula was employed:

$$N_{\text{eff}} \propto \exp(-E_A/kT),$$

where  $k$  is the Boltzmann constant and  $T$  the absolute temperature. As shown in Fig. 3(a), crystal A1 (0.3

TABLE I. Summary of the transport measurements of low resistivity CdSe.

Crystal	Temperature (K)	$\rho$ ( $\Omega$ cm)	$\mu$ (cm <sup>2</sup> /V sec)	$N_{\text{eff}}$ (cm <sup>-3</sup> )	$E_A$ (meV)
A1	300	0.17	880	$4 \times 10^{16}$	22
B	300	0.25	325	$8 \times 10^{16}$	10
A1	80	0.21	2800	$1 \times 10^{16}$	10
B	80	0.13	1500	$2 \times 10^{16}$	10

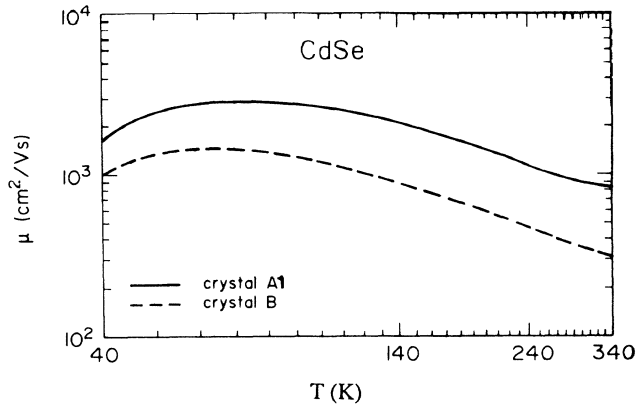


FIG. 2. Electron mobility vs temperature for the two kinds of CdSe crystals (A1 and B).

$\Omega$  cm) exhibited two activation energies:  $E_{A1} = 10$  meV and  $E_{A2} = 22$  meV. One observes that at  $T > 180$  K ( $kT_{180K} = 15$  meV) the deeper donor state is dominant, while below 180 K it is frozen out and only the shallow state is present. The only activation energy measured for crystal B is  $E_A = 10$  meV. Crystal B exhibits very little temperature dependence of  $\mu$  and  $N_{\text{eff}}$  due likely to an overall dominating shallow donor state.

Since this state has an activation energy of 10 meV it

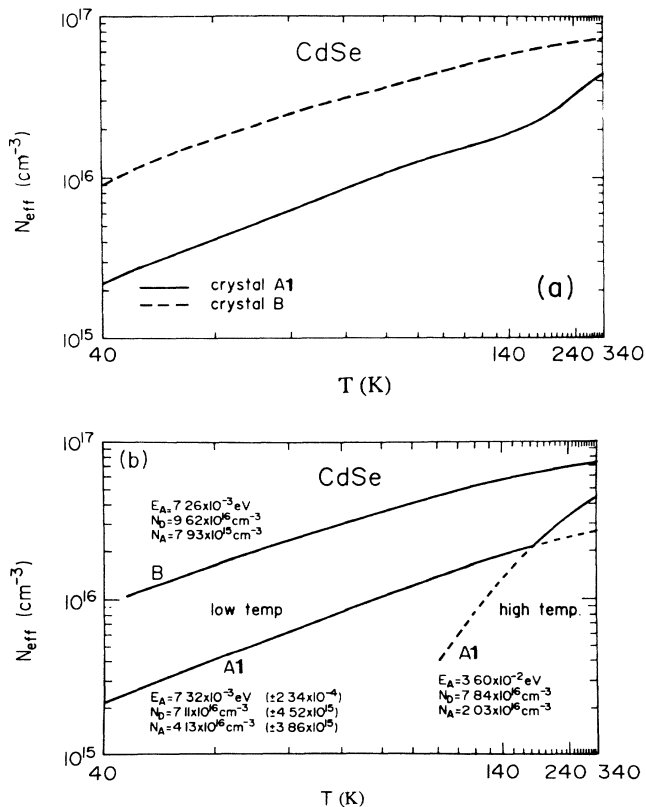


FIG. 3. Free-carrier density vs temperature for the two kinds of CdSe crystals (A1 and B). (a) Measured values. (b) Results of computer simulation.

could not be frozen out in the temperature range of our experiments (down to 40 K;  $kT_{40K} = 3.3$  meV). The deeper state (22 meV) is not observed in crystal B. Presumably the doping density of this donor state is too low in comparison with the shallow state in crystal B.

### B. Secondary-ion mass spectrometry and electron-microprobe measurements

A detailed impurity analysis was carried out for all crystals. Both manufacturers kindly provided us with the impurity analysis of the raw CdSe powder prior to the growth. Whereas the source powder of crystals A contained 23 ppm of Zn as the main impurity, the source powder of crystal B contained 10 ppm of Ca and 9 ppm of Si in the raw material. Additionally, crystals A were specified to have between 1% and 2% sulfur.

SIMS and EM analysis showed that indeed crystals A contained about 1% sulfur, whereas crystal B did not show an appreciable amount of S. It appears that the sulfur had little effect on the measured electronic properties of A crystals. The estimated quantity of Zn in crystal A was below the ppm level using SIMS analysis (no Zn could be detected by EM), and no segregation of any of the impurities or gettering of such impurities in grains or defects was noticed. Since it was expected that alkali atoms serve as the dominant impurities, a careful SIMS analysis with respect to Li and Na was carried out. Li was found to occur much less than Na in all crystals.

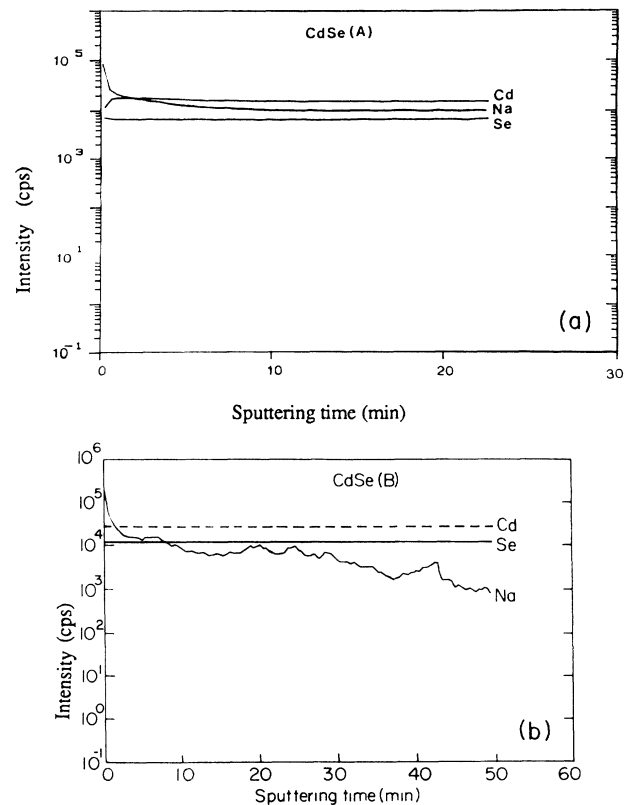


FIG. 4. Concentration profile of Cd, Se, and Na in CdSe (a) crystal A2 and (b) crystal B, obtained via secondary-ion mass spectrometry (SIMS).

TABLE II. Atomic mass counts ratio (bulk) for [Na]/[Cd] (23/111) and [In]/[Cd] (115/111), as determined by SIMS analysis, for various CdSe crystals.

CdSe	$\rho$ ( $\Omega$ cm)	[Na]/[Cd] (count ratio)	[In]/[Cd] (count ratio)
A1	0.3	0.3	0.0011
A2	1	0.3	
A3	11	0.001	
B	0.2	< 0.02	0.0033

Figure 4 shows SIMS profile of crystals A2 and B with respect to the elements Cd, Se, and Na. It is not possible to make any quantitative comparison between the various impurities in the two crystals. However, the [Na]/[Cd] count ratio (in the bulk) was calculated for the various CdSe crystals; the results are given in Table II. It is observed that this ratio increases with the conductivity (1/resistivity) in crystal A. In general, the Na distribution in crystal B was found to be nonuniform, indicating that the sample is not homogeneous (see below). However, if one disregards the surface it is noticed (Fig. 4 and Table II) that the bulk [Na]/[Cd] ratio is larger for crystals A1 and A2 than for crystal B.

Crystal B exhibited also appreciable quantities of Si and Ca impurities in the bulk as well as some impurities (e.g., Cu, K, Zn, Fe, etc.) that were not present in crystal A at all. Both crystal A1 (0.3  $\Omega$  cm) and crystal B contained an appreciable amount of In, which is known to be a shallow donor in CdSe.<sup>18</sup> The bulk [In/Cd] ratio for both crystals is given in Table II.

### C. Photoluminescence measurements

The photoluminescence of the crystals, at various temperatures and under different light intensities, has been measured. At 2 K (Fig. 5) the spectrum of crystal A2 (1  $\Omega$  cm) (Fig. 5) is dominated by two kinds of emission lines: donor-bound exciton at 1.821 eV,<sup>8,9</sup> and a series of broad emission bands having the first peak at 1.732 eV.<sup>7</sup> Under weaker illumination intensity (not shown) this peak exhibited a further red shift to 1.730 eV. These

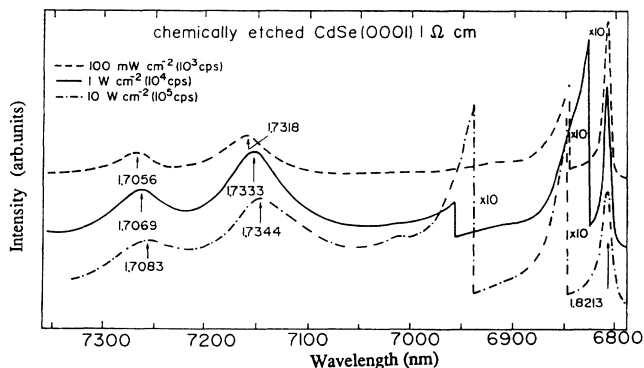


FIG. 5. Photoluminescence of CdSe crystal A2 at 2 K. Excitation wavelength was 514.4 nm. Numbers designating the peaks are in eV.

broad emission lines can be assigned to a donor-acceptor pair (DAP) and its longitudinal-optical-(LO)-phonon replica.

The photoluminescence of crystal A1 in this temperature is shown in Figs. 6(a) and 6(b). The simple excitonic emission of the previous sample is turned into a multi-

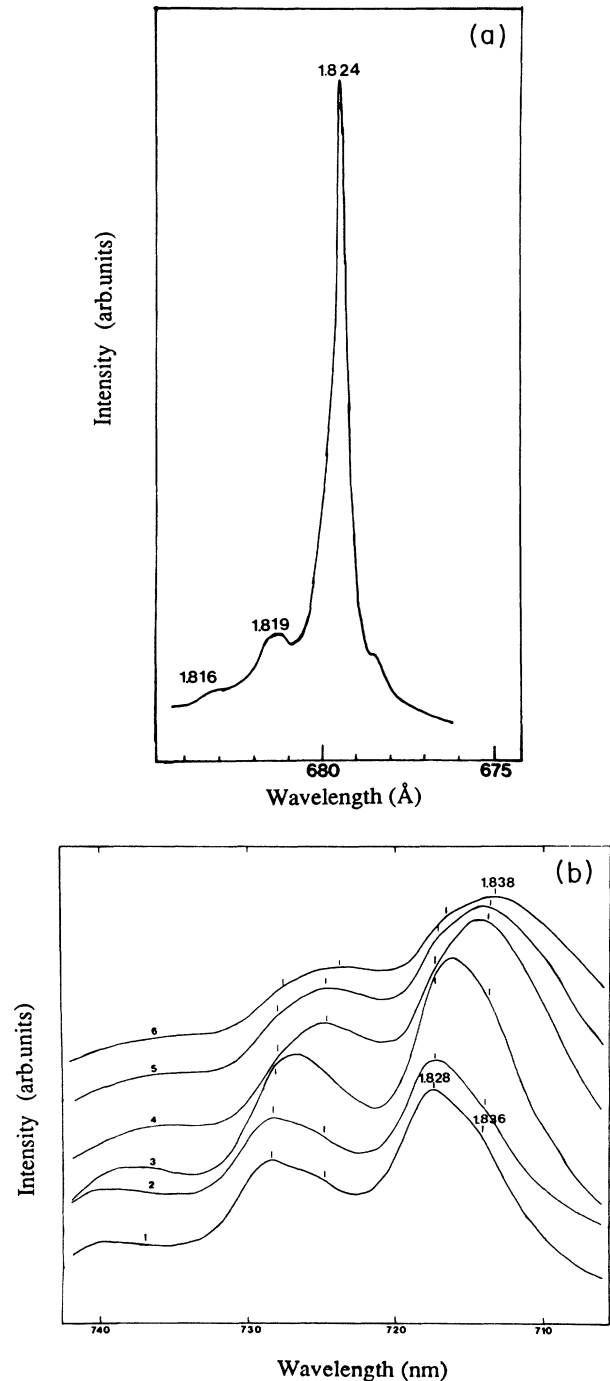


FIG. 6. Photoluminescence of CdSe crystal A1 (0.3  $\Omega$  cm) at 2 K: (a) the excitonic part of the spectrum; (b) donor-acceptor transitions. Excitation wavelength was 514.5 nm. Light intensities (in  $\text{mW cm}^{-2}$ ): 1, 1.2; 2, 6.3; 3, 63; 4, 630; 5, 1800; 6, 5000. Numbers designating the peaks are in eV.

tude of relatively narrow lines in this sample [Fig. 6(a)]. We attribute the line at 1.816 eV to an acceptor-bound exciton ( $I_1$ ).<sup>18</sup> Another weak line at 1.819 eV can be ascribed to a donor-bound exciton ( $I_2$ ). The red shift of 2 meV is likely to be associated with the heavy doping. The strongest line at 1.824 eV is attributed by us to an exciton bound to an ionized donor.<sup>18</sup> A careful inspection of this peak (logarithmic plot) reveals that it is asymmetric and can be deconvoluted into two peaks—one at 1.824 eV, the other at 1.823 eV. This indicates that there are actually two donor states in this material. The donor-acceptor transitions of the A1 sample at various light intensities are shown in Fig. 6(b). Clearly, two donor-acceptor transitions can be resolved. At weak light intensities a deep donor-acceptor transition (1.728 eV) is favored, while a shoulder is clearly observed at 1.736 eV. Under strong light intensity the shallower donor-acceptor transition (1.738 eV) is favored. Note that both transitions exhibit a similar blue shift when the light intensity is increased. These results substantiate the Hall measurements, according to which two shallow donor states exist in this material, with an energy difference of about 10 meV. Crystal B, on the other hand, exhibits a much more complicated pattern. Its luminescence spectrum is not the same over the entire area for one thing. Additionally, it was found that excitation with a long wavelength (647.1-nm Kr<sup>+</sup> laser line) and strong excitation intensity produces more uniform spectra than weak excitation with short wavelength (514.4 nm). No such effect could be reckoned in A crystals. Since the energy of the Kr<sup>+</sup>-ion laser (1.916 eV) is close to the band gap of CdSe at 2 K (1.841 eV), the penetration of the light is deep in this case, and the emission is less influenced by any surface effect. The strong light intensity tends to saturate transitions associated with very dilute impurities, as well as other deep states.

Using the long-wavelength (641.1-nm) excitation for crystal B [Fig. 7(b)], a broad emission was observed at 1.7475 eV followed by a few LO replicas, which can be ascribed to a DAP recombination. The second peak in that series (DAP-LO) (and the lower-energy peaks as well) is broadened. This broadening is probably due to another series of DAP transitions at lower energy. In fact, a series having its first peak at 1.709 eV was observed in this crystal, at selectively illuminated regions, under weak excitations. As the light intensity was increased [Fig. 7(a)], the DAP peak exhibited a blue shift equivalent to about 1 meV/decade, which is typical for donors with large Bohr radius.<sup>15(b)</sup> The relatively high energy of the DAP emission can be attributed to the high excitation intensity used in these experiments.

A series of relatively narrow peaks is observed at higher energies. The main peak in this series at 1.832 eV is attributed (as in crystal A1) to an exciton bound to an ionized donor. The weaker transition at 1.824 eV can be assigned to an exciton bound to a neutral donor. Both transitions suffer a shift to higher energies, likely due to the strain in the crystal. The LO replicas of these two transitions are also observed at 1.804 and 1.799 eV [Fig. 7(a)], respectively. Note that the intensity ratio for the two original lines (1.832 and 1.824 eV) is inverted in the

LO replica (1.804 and 1.799 eV), i.e., the stronger peak in the replica is the exciton bound to a neutral donor. Note also that crystal B does not show any emission that can be attributed to an acceptor-bound exciton (contrary to crystal A1). This observation is associated with the smaller Na impurities, observed in this crystal, which serve as a substitutional acceptor in II-VI materials.<sup>7,15</sup>

In Fig. 8(a) the photoluminescence of crystal A2 is shown at 60 K, while that of crystal B (61 K) is shown in Fig. 8(b). The high-energy side of the photoluminescence spectrum of crystal A2 [Fig. 6(a)] consists of a relatively broad peak (1.811 eV). Using a coefficient of  $2.8 \times 10^{-4}$  eV/K for the shrinkage of the energy gap of CdSe with temperature in this domain,<sup>18</sup> a gap of 1.824 eV is calculated at 60 K, indicating that the above peak is a mixture of the band-to-band and donor-bound-exciton transitions. The series of lower-energy transitions beginning at 1.735 eV are the DAP's and their corresponding phonon replica. It was observed before<sup>7,19</sup> that the donor-acceptor peak of CdSe exhibits a slight blue shift, upon increasing the temperature, up to about 60 K. The spectrum of crystal B consists of three high-energy peaks at 1.835, 1.827, and 1.810 eV, and a DAP at 1.753 eV (possibly the

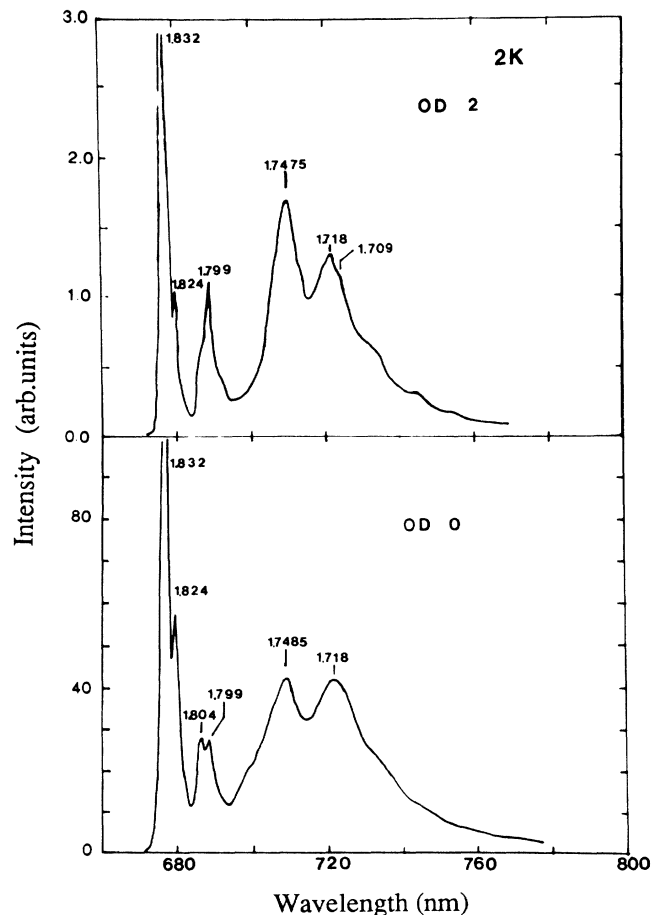


FIG. 7. Photoluminescence of CdSe crystal B at 2 K. Excitation wavelength is 647.1 nm. Light intensities: OD, 0–1.2 MW cm<sup>-2</sup>; OD, 2–12 KW cm<sup>-2</sup>. Numbers designating the peaks are in eV. OD denotes optical density.

latter is mixed with a free-electron-to-bound-hole transition). It is noticed that the difference between the DAP energies of the two crystals increased (18 meV) at 60 K, compared with 2 K (13 meV). This increase is consistent with the observation that the DAP transition in crystal B is produced by a shallower donor than in crystal A2. Thus, by increasing the temperature the donor in crystal B ionizes easier and the DAP transition is mixed with a free-to-bound transition at 60 K. We attribute the

1.835-eV peak to the B gap ( $\Gamma_{7v}-\Gamma_{7c}$ ) and the 1.827-eV peak to the A gap ( $\Gamma_{9v}-\Gamma_{7c}$ ). The 1.810-eV shoulder is a LO replica of the first transition. The second LO replica of this transition at 1.783 eV is observed under strong excitation only.

To determine the activation energy ( $E_A$ ) for the dissociation of the donor state, the photoluminescence of crystal A2 at various temperatures was measured. We use<sup>20</sup>

$$I = I_0 \frac{I}{1 + \exp(-E_A/kT)},$$

where  $I$  and  $I_0$  are the heights of the donor-acceptor peaks at a given temperature and at some reference temperature, respectively. Plotting  $\ln(I_0/I - 1)$  versus  $1/T$ , the activation energy can be determined from the slope. Using this method the activation energy for the DAP of crystal A2 (1  $\Omega$  cm) was determined to be 17 meV.

The photoluminescence of crystal A2 at 140 K consists of a peak at 1.781 eV, which can be ascribed to a band-to-band recombination, while that of crystal B consists of a shoulder (1.826 eV) and a peak (1.798 eV). The 1.798-eV peak is ascribed to a recombination from the A gap, while the 1.826-eV peak can be associated with a luminescence from the higher (B) ( $\Gamma_{7v}-\Gamma_{7c}$ ) gap, which is higher by 25 meV from the A ( $\Gamma_{9v}-\Gamma_{7c}$ ) gap.<sup>18</sup> Whereas the lowest transition (A) can be excited by  $E||c$  light, both A and B gaps can be excited by  $E||c$  light. This transition is enhanced in crystal B likely due to the fact that the crystal orientation is tilted from the  $c$  axis (see below).

Figure 9 shows the temperature dependence of the two main photoluminescence peaks of crystal B. Both peaks exhibit the same temperature shift ( $4.56 \times 10^{-4}$  eV/K) and they are separated by about 26 meV. This observation suggests that they can be associated with the two lower transitions of CdSe (the A and B gaps).

#### D. Spectral response

Photocurrent spectra were measured at room temperature. They were analyzed using the modified Gärtner model.<sup>21</sup> The results of the analysis are shown in Fig. 10. The band gaps of the two crystals are 1.704 and 1.711 eV

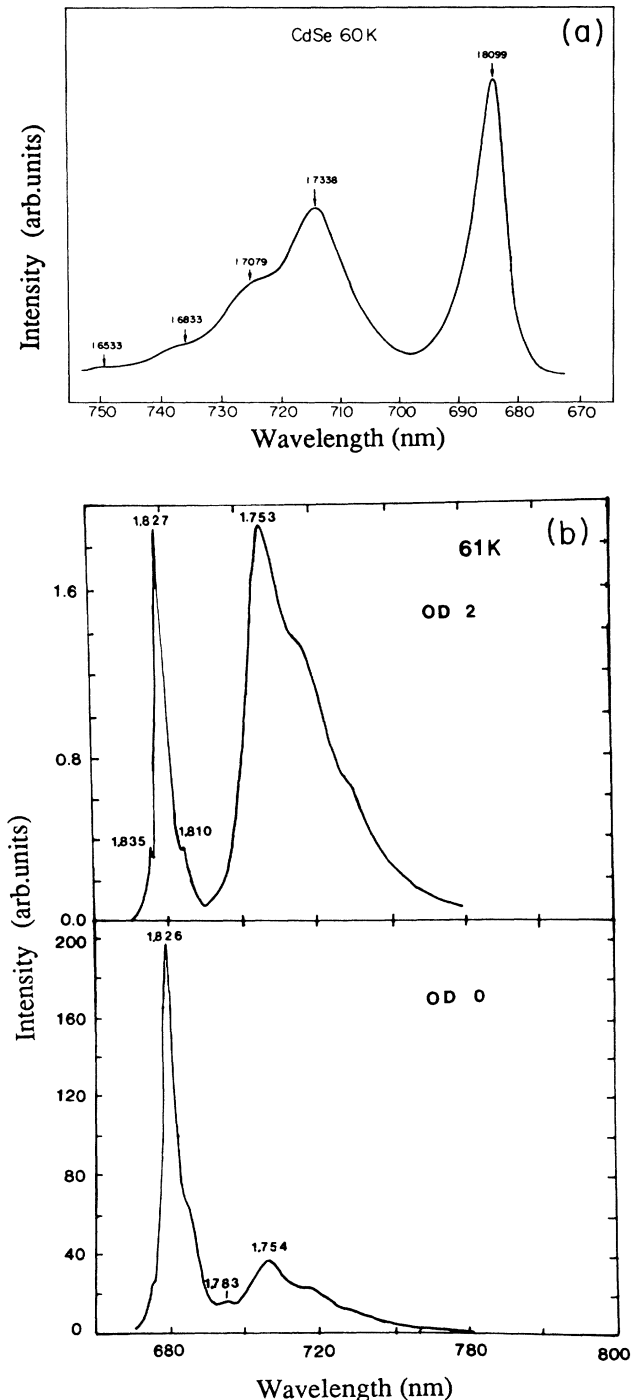


FIG. 8. Photoluminescence of CdSe crystals at 60 K: (a) A2 (0.3  $\Omega$  cm); (b) B. Numbers designating the peaks are in eV.

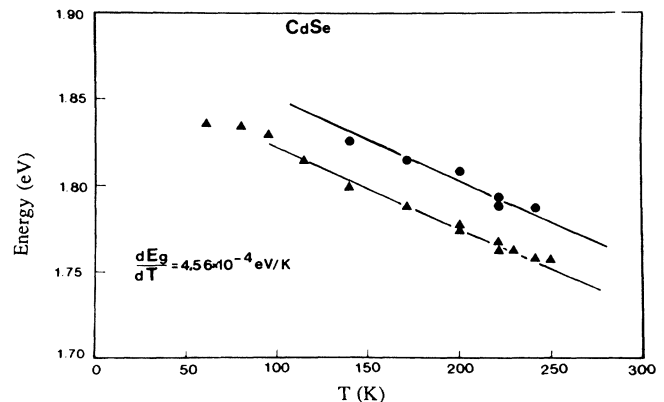


FIG. 9. Temperature dependence of the two photoluminescence maxima in crystal B.

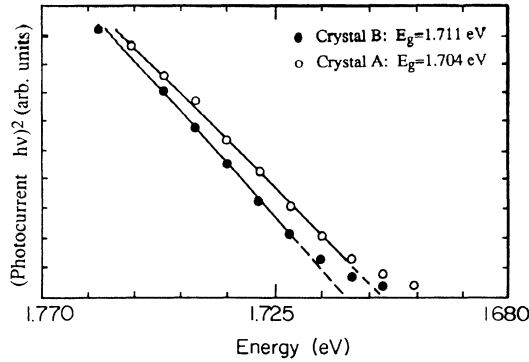


FIG. 10. Band-gap analysis at room temperature obtained from photocurrent measurements of the two kinds of CdSe crystals (1- $\Omega$  cm A2 and B).

for crystals A2 (A1) and B, respectively. Since the slope in this figure is proportional to  $1/N_D^{1/2}$ , it can be concluded that the free-carrier density of crystal B is higher than that of crystal A2. Notice, however, that the room-temperature gap determined from the photocurrent measurements is smaller than that determined from the peak of the photoluminescence measurements at room temperature (1.730 and 1.750 eV for crystal B).

It is also worth mentioning that the photoresponse of A crystals in a solution of polysulfide electrolyte was superior to that of crystal B. After photoelectrochemical etching (photoetching) the photoresponse of the two crystals increased for supra-band-gap illumination and it exhibited a red shift of a few meV.<sup>22</sup> Crystal A2 exhibited a better photoresponse than crystal B after photoetching, although the difference between the two crystals was not as large as before photoetching. It was noticed before<sup>22(b)</sup> that, while the improvements in the photoresponse of high-quality crystals is rather modest after photoetching, substantial improvements are obtained with lower-grade materials. This effect could be explained by the refraction of the light impinging on a textured surface, which produces a larger enhancement in the photoresponse for materials with small minority-carrier diffusion length.

#### E. X-ray diffraction

To try to understand the reasons for the marked differences between the optical properties of crystals A2 and B, a detailed x-ray investigation was carried out on both type of crystals in the Laue mode. Crystal A2 exhibited a high-quality diffraction pattern with hexagonal symmetry typical of the (0001) face of this crystal. Furthermore, rocking curves were taken for this kind of crystal. The full width at half maximum was found to be of the order of 10 arcsec, which attests for the quality of the A crystals. Crystal B exhibited an hexagonal diffraction pattern, but much less regular. First, in a number of selectively irradiated regions, on each of two analyzed B samples, there was a clear evidence for the presence of more than one crystallite in the irradiated zone (1 mm). Furthermore, the symmetry of the diffraction image was not always reproducible. In some

cases four-axis symmetry was observed. Additionally, in a few zones the diffraction dots were not sharp, which was interpreted as an evidence for strain in the crystal. Fractures of crystal B were examined as well. It was found that some of the fractures contained planes which deviated  $13^\circ$  from the (0001) hexagonal face.

#### IV. DISCUSSION

Regarding the transport measurements, both kind of crystals show the same power law in the temperature range between 130 and 340 K for the mobility versus temperature. The exponent  $n = -1.15$  shows that the scattering mechanism is not purely by acoustic phonons, which would yield  $n = -1.5$ .<sup>23</sup> In polar semiconductors scattering by optical phonons exists too. At high temperatures variation of the mobility due to scattering by optical phonons behaves like  $T^{-1/2}$ .<sup>24</sup> The combined mobility adds up reciprocally. It appears that the dominant scattering mechanism in the high-temperature range is the scattering by acoustic and optical phonons.<sup>5</sup> At low temperatures scattering by ionized impurities predominates. The temperature range available in these measurements was too small to permit the determination of the slope. However, it is noticed that the mobility of crystal A1 is higher than that of crystal B, which is in agreement with the observation that the concentration of ionized impurities is larger in the latter case.

As one can see from Table I, the transport properties indicate that the density of free carriers is larger in crystal B than in crystal A1, and the mobility of the electrons in crystal B is inferior to that in crystal A1. In addition, the x-ray Laue measurements show that crystal B is actually not a single crystal and that it has many irregularities in the lattice.

In order to analyze our data we have fitted the temperature dependence of the free carriers [Fig. 3(a)] to the following model:<sup>25</sup>

$$\frac{n(n - N_A)}{N_D - N_A - n} = \frac{1}{D} \frac{2(2\pi m^* kT)^{3/2}}{h^3} \exp(-E_A/kT),$$

where  $n$  is the free-carrier concentration,  $D$  the degeneracy ( $=2$ ),  $N_A, N_D$  the density of acceptors and donors, respectively,  $m^*$  the effective mass of electrons ( $=0.13m_e$ ), and  $E_A$  the activation energy of electrons.

The results of the computer fit are shown in Fig. 3(b). A satisfactory agreement with the experimental data was obtained using the parameters given in Table III. It is noticed that the density of free carriers is larger in crystal B than in crystal A1 for all temperatures, as indicated by the experiments. In crystal A1 the fit could be achieved only if two separate regimes were assumed. At low temperatures the behavior of the free-carrier density was dominated by the ionization of a shallow donor (7.3 meV), while the high-temperature behavior was dominated by the ionization of a deeper donor (36 meV). The transport measurements suggest that two kind of shallow donors exist in CdSe crystals of that kind: a very shallow donor of energy of about 7–10 meV and a deeper one (22–36 meV). It is important to note that 7–10-meV level is the shallowest impurity level reported for CdSe (to the

TABLE III. Results of computer calculations of free-carrier density as a function of temperature.

Crystal	A1 (low temp.)	A1 (high temp.)	B
$N_A$ ( $\text{cm}^{-3}$ )	$4.13 \times 10^{16}$	$2.03 \times 10^{16}$	$7.93 \times 10^{15}$
$N_D$ ( $\text{cm}^{-3}$ )	$7.11 \times 10^{16}$	$7.84 \times 10^{16}$	$9.62 \times 10^{16}$
$E_A$ (meV)	7.3	36.0	7.3
$K = N_A/N_D$	0.58	0.25	0.08

best of our knowledge). Very shallow levels of interstitial alkali atoms were observed in ZnSe.<sup>14</sup> Group-III and -VII impurities were identified as somewhat deeper donors in ZnSe.<sup>14</sup>

The major contaminants in the source powder of crystal A are S (1%) and Zn (23 ppm), which are isoelectronic with Se and Cd, respectively. The source material of crystal B contained some Ca (10 ppm) and Si (9 ppm). These contaminants are not known to have shallow levels in CdSe and they were not found in substantial quantities by SIMS analysis.

The photocurrent spectra presented in Fig. 10 show that the band gap of crystal B is larger by 8 meV from that of crystal A. The broadening of the gap for crystal B could be attributed to a Burstein-Moss shift,<sup>26,27</sup> or to the existence of a strain in crystal B. Using the free-carrier densities of the two crystals (Table II) and the effective mass of the electron ( $0.13m_e$ ),<sup>18</sup> one can expect that crystal B will exhibit a gap larger by 2 meV than that of crystal A2. The first possibility can be ruled out, however, as indicated from the low-temperature photoluminescence measurements. First, the bound exciton of crystal B is 3 meV higher in energy than the expected position (1.824 instead of 1.821 eV) at 2 K; second, the peak of the band-to-band transition in the photoluminescence measurements (effective band gap) is higher in crystal B than in crystal A2 at 140 K. This suggests that the difference in band gap persists also at low temperatures and is independent of the density of free carriers, as would be expected from the Burstein-Moss theory. It emerges therefore, that the difference in the band gaps of the two crystals can be attributed to the strain in crystal B, and to the deviation of crystal B face from the (0001) plane, which was verified experimentally through x-ray Laue measurements.

Crystal B shows a weak exciton peak at 1.824 eV, besides the strong 1.832-eV line. The former line might have the same origin as the 1.821-eV line in crystal A ( $I_2$ ), but shifted due to stress. This interpretation is supported by the transport measurements, which indicate that the concentration of the deeper donor (20 meV) in crystal B is at least 1 order of magnitude lower than in crystal A1. The peak at 1.832 eV in crystal B is assumed to originate from a recombination of an exciton bound to an ionized donor, again shifted to higher energy due to the inner stress in the crystal. This identification is supported by the reversing of the intensity ratio of the LO replica of the two peaks. The exciton bound to a neutral donor is expected to have stronger interaction with the optical phonons than excitons bound to ionized donors,

and hence the inversion of the intensity ratio in the LO replica. The high doping level of crystal A1 produces strong donor-donor interaction, which leads to a higher ratio of densities of ionized donor to neutral donor than in crystal A2. Therefore, the luminescence of crystal A1 (and B) is dominated by an exciton bound to an ionized donor, while in crystal A2 the luminescence of excitons bound to neutral donors is prevalent.

Considering now the donor-acceptor pair luminescence. Crystal A2 (1  $\Omega$  cm) exhibits a spectrum similar to that found in Refs. 7 and 8 for CdSe, which has been annealed in NaCl atmosphere (B1 band). In Ref. 28 a similar spectrum was obtained for crystals which were grown from the vapor phase. In Ref. 7 the authors argue that the donor state in this case is a  $\text{Cl}_{\text{Se}}$  atom (Cl at a Se site) and the acceptor state is assigned to  $\text{Na}_{\text{Cd}}$ . The donor energy is assumed to be 19 meV,<sup>7</sup> which is comparable to the activation energy of the deeper donor of this study as concluded from the photoluminescence and transport measurements. The energy of the DAP luminescence peak (under weak excitation) in Ref. 7 is 1.7325 eV. The value of the fundamental gap of CdSe is 1.841 eV (Ref. 28) at 2K (in Ref. 7 the band gap is overestimated by about 19 meV). Taking these values together, one obtains a rough estimation of the acceptor energy of 85–90 meV (rather than 109 meV in Ref. 7).

The line shape of the DAP of the In-doped A1 crystal (0.3  $\Omega$  cm) varies considerably with light intensity, and is different from that of the 1- $\Omega$  cm (A2) CdSe (see Figs. 5 and 6). In fact, crystal A1 exhibits two donor-acceptor transitions differing by about 10 meV. (The experimental difference between the two transitions, under weak light intensities, is 8 meV. If deconvoluted this difference is likely to be closer to 10 meV.) In Fig. 11 the theory of Neumark *et al.*<sup>15(b),15(d)</sup> is used to calculate the position of the maximum of the donor-acceptor pair as a function of light intensity, for two donor densities, and for two sizes of the Bohr radius. A comparison with the experimental data of crystals A1 and A2 is shown as well. It is found that the maximum of the DAP of crystal A2 varies with intensity in a manner typical of crystals with  $N_D = 1 \times 10^{16} \text{ cm}^{-3}$  (curve 1), while the low-energy donor-acceptor peak of crystal A1 varies with an intensity akin to crystals with  $N_D = 7.5 \times 10^{16} \text{ cm}^{-3}$  (curve 2). It is noticed that the donor densities used for the fitting conform with those provided by the supplier and the Hall measurements. This calculation indicates that the donor-acceptor peak of crystals A2 and the deep donor-acceptor transition in crystal A1 have the same origin. In view of the high [Na]/[Cd] ratio in crystal A2 (and



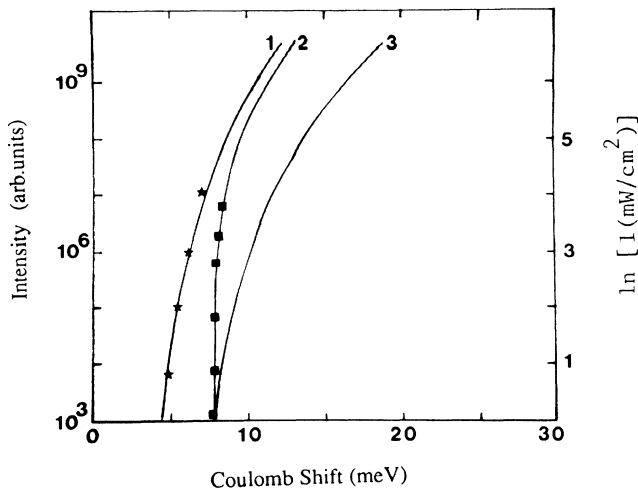


FIG. 11. Analysis of the DAP luminescence from the theory of Newmark *et al.* [Refs. 15(b) and 15(d)]. Curve 1: Bohr radius 40 Å;  $N_D = 1 \times 10^{16} \text{ cm}^{-3}$ . Curve 2: Bohr radius 40 Å;  $N_D = 7.5 \times 10^{16} \text{ cm}^{-3}$ . Curve 3: Bohr radius 24 Å;  $N_D = 7.5 \times 10^{16} \text{ cm}^{-3}$ . ★, experimental results for crystal A2; ■, experimental results for crystal A1.

A1), and the agreement with the literature, it is concluded that this transition can be attributed to a substitutional sodium (acceptor) and interstitial sodium (donor). It is assumed that substitutional sodium ( $\text{Na}_{\text{Cd}}$ ) serves as an acceptor for the two donor-acceptor transitions, and hence the energy difference between the two DAP reflects the difference in the donor energies, under weak illumination.

It has been suggested that acceptor states derived from group-I elements Li and Na take the following energy levels in CdSe: for Li,  $E_V + 0.109 \text{ eV}$ ,<sup>8(b),7</sup> and for Na,  $E_V + 0.109 \text{ eV}$  [Refs. 8(b) and 7] and  $E_V + 0.082 \text{ eV}$ .<sup>18</sup>

Note, however, that in Ref. 7 the sum ( $E_g$ ) of the donor ionization energy plus acceptor ionization energy plus donor-acceptor peak is 1.860 eV, whereas in Ref. 8(b) this sum is 1.847 eV, compared with the experimental value of 1.841 eV.<sup>29</sup> If a correction is made to that energy, then the acceptor energy is  $E_V + 0.089 \text{ eV}$  in Ref. 7 and about  $E_V + 0.100 \text{ eV}$  in Ref. 8(b).

The values obtained for crystal A2 (1 Ω cm) are in good agreement with these data, and hence it is likely that the same kind of donor-acceptor pair transition is involved, i.e.,  $\text{Cl}_{\text{Se}}\text{-Na}_{\text{Cd}}$ , or  $\text{Na}_i\text{-Na}_{\text{Cd}}$ . However, very little amount of Cl was found in crystals A using SIMS measurements; hence the second assignment is preferred. Crystal A1 exhibits two transitions: the deeper one at 1.728 eV likely has the same origin as the DAP pair in crystal A2, i.e.,  $\text{Na}_i\text{-Na}_{\text{Cd}}$ ; the shallower transition at 1.736 eV is likely to be associated with the In shallow donor ( $\text{In}_{\text{Cd}}\text{-Na}_{\text{Cd}}$ ). One can assume a common acceptor for the two DAP transitions ( $\text{Na}_{\text{Cd}}$ ). One can assume a common acceptor for the two DAP transitions ( $\text{Na}_{\text{Cd}}$ ). In that case the difference between the two shallow donor states of 8–10 meV agrees very well with the values deter-

mined by Hall measurements (20 and 10 meV, respectively). Consequently, the acceptor energy is concluded to be 0.095 eV, in good agreement with the values cited above. The DAP transition in crystal B was found to be shallow (1.748 eV) and to vary only little with light intensity, under the strong light intensities used in this experiment. Since this crystal was found to contain much less Na than crystals A, and more In, it can be assumed that the DAP transition of crystal B is of the type  $\text{In}_{\text{Cd}}\text{-Na}_{\text{Cd}}$ . The difference (about 10 meV) between the shallow DAP transition in crystals A1 and crystal B could be attributed to the strain (2–7 meV) present in crystal B, and to the strong excitation intensity. Preferential ordering of the pairs<sup>30</sup> cannot be excluded. Assuming, then, the In to be responsible for the shallow donor level (7–10 meV), and the Na for the deeper level (22–36 meV) it is clear that the transport properties and the photoluminescence of crystals A are dominated by the Na level, while the properties of crystal B are dominated by the In level. A somewhat different situation was found for Na-doped ZnSe.<sup>15(b)</sup> Using a careful analysis of photoluminescence data, it was concluded that interstitial Na constituted the shallow donor states in ZnSe, while the deeper donor-acceptor transition was assigned to In. However, no experimental data are presented as for the variation of the two peaks with light intensity in ZnSe. It is possible that the difference between the spectra of the two crystals emerges from the different crystal structure (ZnSe has cubic structure, while CdSe has wurzite structure). It should also be noticed that the ZnSe crystals were intentionally doped with alkali metals, and the In served (possibly) as a residual impurity, which is the opposite situation in our case (In served as the extrinsic dopant and Na as the residual impurity). Henry *et al.*<sup>8</sup> studied the photoluminescence of Na-, Li-, and In-doped CdS (which has a wurzite structure like CdSe). They concluded that the donor level of In is situated 0.034 eV from the conduction band ( $\text{Ga}$  at  $E_c - 0.033 \text{ eV}$ ). To determine the levels of Na and Li, they doped the CdS crystals with these elements and studied their photoluminescence spectrum. They suggest that interstitial Na and Li are responsible for the donor states. Taking the value of the energy gap of CdS at this temperature as 2.582 eV,<sup>18</sup> the acceptor levels of Na and Li are found by them to be  $E_V + 0.169 \text{ eV}$  for Na and  $E_V + 0.165 \text{ eV}$  for Li; the donor-acceptor transitions are found to be 2.391 eV for Na and 2.397 eV for Li, and one obtains (disregarding any Coulomb shift) for the donor levels of Na and Li the value  $E_c - 0.022 \text{ eV}$ . Thus, in CdS too (as was found for ZnSe) the donor levels of the alkali metals are seemingly shallower than the donor levels of group-III elements. Further experiments are necessary to clarify this point. However, it is possible that other impurities were introduced during the growth process. Since no impurity analysis was done in this case, it is not possible to do any conclusive comparison between the present work and Ref. 8.

Crystals A contains some 1 at. % S, yet they do not exhibit line broadening of the exciton PL lines, which is typical of semiconductor alloys. It was shown<sup>31</sup> that the addition of < 1 at. % Se into CdS does not yield broadening of the free-exciton line in undoped high-

resistivity crystals. Larger concentrations of Se yield potential fluctuations which produce strong localization of the free exciton and broadening of the emission line. In the present study low-resistivity crystals were used and the free-exciton transition was overwhelmed by the deeper bound-exciton transition. Broadening of bound-exciton lines was observed in various II-VI alloys<sup>20</sup> also due to potential fluctuations. No such broadening was observed in crystal A2 (1  $\Omega$  cm) and hence the trapping of excitons in potential fluctuations produced by sulfur atoms is not relevant in this case.

## V. CONCLUSIONS

The optical and electronic properties of Bridgman-grown, low-resistivity CdSe were investigated. They were found to be governed by two donors. A shallow level (10 meV), which was not reported before, and a deeper one (20 meV). The analysis of the data suggests that In is re-

sponsible for the shallow level, while the deeper level is attributed to Na. This is in contrast with recent data on ZnSe. Further experiments are required to understand the reason for the difference between these two closely related crystals.

## ACKNOWLEDGMENTS

We are grateful to C. Grattapain for the SIMS analysis, to J. F. Rommeluere for the photoluminescence measurements, and to M. Rommeluere for the EM analysis. This research was supported in part by a grant from the National Council for Research and Development, Israel, the Bundesministerium für Forschung und Technologie, Federal Republic of Germany, and the French Foreign Office through the DRCI. One of us (R.T.) is a recipient of support from the French Ministry of Science and Technology.

- <sup>1</sup>G. Hodes, in *Energy Resources through Photochemistry and Catalysis*, edited by M. Grätzel (Academic, New York, 1983), Chap. 13.
- <sup>2</sup>I. B. Ermolovich and E. L. Shtrom, *Thin Solid Films* **22**, 157 (1974).
- <sup>3</sup>A. Van Calster, A. Vervae, I. de Bijcke, J. de Beats, and J. Vanfletern (unpublished).
- <sup>4</sup>M. A. Ryan, C. Levy-Clement, D. Mahalu, and R. Tenne, *Ber. Bunsenges. Phys. Chem.* (to be published).
- <sup>5</sup>A. L. Robinson and R. H. Bube, *J. Appl. Phys.* **42**, 5280 (1971).
- <sup>6</sup>R. S. Krupyshev, S. A. Abagyan, A. A. Davydov, and A. A. Karushina, *Fiz. Tekh. Poluprovod.* **6**, 1643 (1972) [*Sov. Phys.—Semicond.* **6**, 1422 (1973)].
- <sup>7</sup>B. M. Arora and W. Compton, *J. Appl. Phys.* **43**, 4499 (1972).
- <sup>8</sup>(a) C. H. Henry and K. Nassau, *Phys. Rev. B* **2**, 997 (1970); (b) C. H. Henry, K. Nassau, and J. W. Shiever, *ibid.* **8**, 2453 (1971); (c) K. Nassau, C. H. Henry, and J. W. Shiever (unpublished).
- <sup>9</sup>(a) E. F. Gross, B. S. Razbirin, V. P. Fedorov, and Yu. P. Naumov, *Phys. Status Solidi B* **30**, 485 (1985); (b) P. Y. Yu and C. Hermann, *Phys. Rev. B* **23**, 4097 (1981).
- <sup>10</sup>A. K. Arora and A. K. Ramdas, *Phys. Rev. B* **35**, 4345 (1987).
- <sup>11</sup>R. Garuthara, M. Tomkiewicz, and R. Tenne, *Phys. Rev. B* **31**, 7844 (1985).
- <sup>12</sup>R. Tenne, H. Mariette, C. Levy-Clement, and R. Jäger-Waldau, *Phys. Rev. B* **36**, 1204 (1987).
- <sup>13</sup>D. L. Rosen, Q. X. Li, and R. R. Alfano, *Phys. Rev. B* **31**, 2396 (1985).
- <sup>14</sup>M. Aven, in *II-VI Semiconducting Compounds*, edited by D. G. Thomas (Benjamin, New York, 1967), p. 1232.
- <sup>15</sup>(a) R. N. Bhargava, R. J. Seymour, B. J. Fitzpatrick, and S. P. Herko, *Phys. Rev. B* **20**, 2407 (1979); (b) G. F. Neumark, S. P. Herko, and B. J. Fitzpatrick (unpublished); (c) G. F. Neumark, S. P. Herko, T. F. McGee III, and B. J. Fitzpatrick, *Phys. Rev. Lett.* **53**, 604 (1984); (d) G. F. Neumark, *Phys. Rev. B* **37**, 4778 (1988).
- <sup>16</sup>(a) J. Reichman and M. Russak, *J. Electrochem. Soc.*, **128**, 2053 (1981); (b) M. Tomkiewicz, I. Ling, and W. S. Parsons, *ibid.* **129**, 2016 (1982).
- <sup>17</sup>(a) J. Rioux, *Bull. Soc. Fr. Mineral. et Cristallogr.* **LXXXIX**, 329 (1966); (b) J. Rioux, Centre National de la Recherche Scientifique Patent No. 1401261.
- <sup>18</sup>*Semiconductors*, Vol. 17 of *Landolt-Börnstein: Functional Relationships in Science and Technology*, edited by K. H. Hellwege (Springer-Verlag, Berlin, 1982), p. 202.
- <sup>19</sup>R. Tenne, H. Mariette, C. Levy-Clement, and R. Jäger-Waldau, *J. Cryst. Growth* **86**, 826 (1988).
- <sup>20</sup>C. Uzan, H. Mariette, and A. Muranevich, *Phys. Rev. B* **34**, 8728 (1986).
- <sup>21</sup>Yu. V. Pleskov and Yu. Ya. Gurevich, *Semiconductor Photoelectrochemistry* (Consultants Bureau, New York, 1986), p. 183.
- <sup>22</sup>(a) R. Tenne and G. Hodes, *Appl. Phys. Lett.* **37**, 428 (1980); (b) R. Tenne, D. Mahalu, E. Klein, and W. Giriat, *Solar Energy Mater.* **17**, 65 (1988).
- <sup>23</sup>(a) S. M. Sze, *Physics of Semiconductor Devices* (Wiley, New York, 1981), p. 28; (b) P. P. Debye and E. M. Conwell, *Phys. Rev.* **93**, 693 (1954).
- <sup>24</sup>S. S. Delvin, in *Physics and Chemistry of II-VI Compounds*, edited by M. Aven and J. S. Prener (North-Holland, Amsterdam, 1967), p. 561.
- <sup>25</sup>J. H. DeBoer and W. C. van Geel, *Physica* **2**, 186 (1935).
- <sup>26</sup>H. Jäger and E. Seipp, *J. Appl. Phys.* **52**, 425 (1981).
- <sup>27</sup>R. Tenne, H. Flaisher, and R. Triboulet, *Phys. Rev. B* **29**, 5799 (1984).
- <sup>28</sup>D. C. Reynolds, C. W. Litton, and T. C. Collins, *Phys. Rev.* **156**, B881 (1967).
- <sup>29</sup>R. G. Wheeler and J. O. Dimmock, *Phys. Rev.* **125**, B1805 (1962).
- <sup>30</sup>P. J. Dean, in *Progress in Solid State Chemistry*, edited by J. O. McCaldin and G. Somorjai (Pergamon, New York, 1973), Vol. 8, pp. 1–126.
- <sup>31</sup>S. Permogorov, A. Reznitski, S. Verbin, G. O. Müller, P. Flögel, and M. Nikiforova, *Phys. Status Solidi B* **113**, 589 (1982).